Available online at www.sciencedirect.com
SCIENCE DIRECT
ELSEVIER
Polymer 46 (2005) 2748–2757
polymer
www.elsevier.com/locate/polymer

Crystalline organization and toughening: example of polyamide-12

Laurent Corté[a], François Beaume[b], Ludwik Leibler[a,*]

[a]Matière Molle et Chimie, Ecole Supérieure de Physique Chimie Industrielle (UMR ESPCI-CNRS 167), 10 rue Vauquelin 75231 Paris Cedex 05, France
[b]CERDATO, ARKEMA, 27470 Serquigny, France

Received 15 November 2004; received in revised form 6 January 2005; accepted 7 January 2005

Abstract

Improving the impact resistance of plastics is a key to many applications. Today, dispersing rubber and inorganic particles into semicrystalline polymers is widely used to increase their impact strength without greatly altering other interesting properties such as elastic modulus or chemical resistance. Yet, the underlying mechanisms controlling such toughening are controversial. Hitherto it has been often suggested that a critical distance between particles which controls the brittle-to-tough transition is an intrinsic property of the polymer. On the contrary, we demonstrate here that differences in crystalline organization of the matrix can induce dramatic changes in toughening efficiency. A thermal treatment and microscopic observations strongly suggest that crystalline orientation, size of crystalline grains and molecular organization at grain boundaries play a determinant role in the toughening mechanisms. These observations may have important implications for designing and manufacturing tough plastic materials.

Keywords: Toughening; Polyamide; Semi-crystalline polymers

1. Introduction

The impact resistance of semicrystalline polymers such as polyolefins or polyamides, is dramatically affected by the presence of defects or sharp notches which act as stress-concentrators and favor brittle fracture. In the past 50 years, great research efforts have been carried out to reduce the defect-sensitivity and improve the impact strength of these materials. Within this context, it was found that semicrystalline polymers can be considerably toughened by dispersing a second phase—usually rubber—in the semicrystalline matrix [1,2]. For instance, incorporating 20% of ethylene–propylene rubber particles into a polyamide-6 matrix can lead to a 10-fold increase in the impact resistance of notched specimens [3]. Such toughened semicrystalline plastics are now widely used in a large variety of demanding industrial applications ranging from automotive parts to off-shore pipes. Here, we present microscopic observations of toughened systems which bring a new insight into the mechanisms underlying the toughening of semicrystalline polymers.

In a very schematic way, the toughening strategy consists in modifying the polymer material to dissipate the impact energy by other means than crack propagation. In semi-crystalline polymers toughened with particles, both experimental [4–11] and theoretical [12–16] studies show that toughening results from a multiple step mechanism where cavitation and plastic deformation are crucial. When a crack propagates through an efficiently toughened system, voids are created inside or around the particles due to strong stress concentration at the front of the advancing crack. Particle cavitation and void formation generates a new stress distribution in the material which facilitates the initiation of plastic deformation of the matrix. As a consequence, the matrix ligaments confined between cavitated particles can undergo extensive plastic deformation which dissipates large amount of impact energy. The succession of particle cavitation, the initiation step, and matrix plastic deformation, the dissipative one, are now well-admitted mechanisms. However, the molecular parameters controlling their activation have not yet been clearly identified. The ability to predict toughening efficiency remains a controversial and challenging issue.

* Corresponding author. Tel.: +33 1 40 79 51 22; fax: +33 1 40 79 51 17.
E-mail address: ludwik.leibler@espci.fr (L. Leibler).

0032-3861/$ - see front matter © 2005 Elsevier Ltd. All rights reserved.
doi:10.1016/j.polymer.2005.01.040

Abundant literature has focused on the influence of particle dispersion on the impact resistance of toughened semicrystalline polymers. A first study by Wu on toughened systems of polyamide-6,6 indicates that toughening efficiency strongly correlates with the average ligament thickness, L_n, which is defined as the average surface-to-surface distance between two neighbored particles [17]. Such a length characterizes the confinement of the matrix. Experimentally, it is controlled by varying the concentration and size of the filler particles. In his work, Wu reports that for given temperature and impact conditions, extensive plastic deformation of the matrix is possible when L_n is lower than a critical value, L_c. Several groups have reported later the existence of a similar critical length in other matrices (polyamide-6 [3,19], highdensity polyethylene [20,21], isotactic polypropylene [18], polyethylene terephthalate [22]) using various rubber [3,17–20,22] and inorganic [21] fillers. For a given polymer matrix, this critical length, L_c, seems to be constant independently of the nature of the filler particles, filler content and particle size. Thus, it has been suggested that there exists a characteristic confinement length intrinsic to each semicrystalline polymer determining the onset of toughening efficiency. For instance, toughening at room temperature and under standard impact conditions should only be successfully achieved for L_n values lower than 300 nm in polyamide-6,6 [17] or 600 nm in high-density polyethylene [21], whatever the fillers are.

The microscopic picture proposed to explain the existence of an intrinsic critical confinement thickness, L_c, relies on the presence of highly oriented crystalline layers wrapping each particle with a well-defined thickness of about half L_c [6]. Due to their crystalline orientation, these so-called transcrystalline layers would exhibit a strong anisotropic behavior with directions of low shear yield stress parallel to the particle surface. In consequence, for ligament thickness lower than L_c, transcrystalline layers would percolate through the whole material enabling extensive plastic deformation of the matrix and high levels of toughness. Numerical mechanical models confirm that transcrystalline layers favor the plastic deformation of the matrix and indeed could bring toughness [16]. Experimentally, however, such layers have been observed in polyamide thin films prepared by spin-coating from solutions [6] but no studies have been reported for bulk samples. Here, we present transmission electron microscopy studies of bulk toughened polyamide-12 showing that there is no transcrystalline layers around particles. In injected samples, the crystalline organization of the matrix happens to be strongly determined by the processing conditions and particularly the local flow direction. In addition, this crystalline organization can be modified by a thermal treatment which also dramatically affects the toughening efficiency. Such processing and thermal history dependence suggests that the concept of an intrinsic critical length, although appealing, is very questionable.

2. Experimental

2.1. Materials

Semicrystalline polyamide-12 with $M_n = 25{,}000$ and $I_p = 2.3$ was provided by Arkema. Two impact modifiers were studied at various concentrations ranging from 0 to 30 wt%: reactive ethylene/propylene rubber (EPR*) and poly(styrene)-*block*poly(butadiene)-*block*-poly(methyl methacrylate) triblock terpolymer (SBM). Blending was achieved by extruding together the modifier and the semicrystalline matrix. Different particle dispersions were obtained by varying the concentrations and extruding conditions. In the case of EPR* which is very reactive, particle diameters are small (~50–100 nm) and quite monodisperse. In SBM toughened systems, particle sizes are much larger (~0.1–1 μm) and more polydisperse. More details about the use of SBM as an impact modifier will be published elsewhere [23]. Compositions and number average particle diameter, d_n, are given in Table 1 for some representative systems.

2.2. Processing and thermal treatment

Impact test bars were injected according to ASTM/ISO requirements. A thermal treatment was applied to some of the injected samples as follows. Test bars were first melted at 200 °C for 20 min in a mould and under a press to avoid contact with air. Melted bars were then slowly cooled under the press down to room temperature (1 °C/min). All the bars were dried in a vacuum oven at 50 °C for 24 h prior to this treatment and kept in a desiccator until they were tested. Notches were cut according to the specifications of ISO179, after the treatment and just before impact testing.

2.3. Characterization

Optical micrographs were obtained under crossed polarizers from thin (~5 μm) microtomed sections on a LEITZ DMRXE microscope.

Particle dispersions and matrix crystalline organizations were characterized by transmission electron microscopy (TEM) using stained ultrathin sections. Ultrathin sections were cut by ultramicrotomy with a diamond knife at −100 °C. Osmium tetroxide (OsO_4) vapor was used to selectively stain SBM particles in PA12/SBM systems. An aqueous solution of phosphotungstic acid (H_3PO_4, $12WO_3$) and benzyl alcohol was used to stain the polyamide matrix and reveal the crystalline lamellae [24]. Benzyl alcohol acts as a dyeing assistant and helps diffusion of WO_3 which preferentially stains the amorphous polyamide layers. Experiments were carried out with a JEOL 100CX electron microscope at an acceleration voltage of 80 kV. For each blend, particle size distribution was obtained by image analysis with the ImageJ software [25] on 200–800 particles and over several tens of μm^2. The diameter, d, of each particle was estimated by:

Table 1
Samples characteristics. Particle dispersions are characterized by the standard deviation s of the log-normal fit, the number average particle diameter, d_n, and the number average interparticle ligament thickness, L_n

Materials description			Particle dispersion		
Blend reference	Filler content	History	s	d_n, nm	L_n, μm
Neat PA12	0 wt%	Injected	–	–	–
		Recrystallized	–	–	–
1	10 wt% EPR*	Injected	0.55	85	0.13±0.02
		Recrystallized	0.34	96	0.11±0.02
2	20 wt% EPR*	Injected	0.26	110	0.07±0.02
		Recrystallized	0.28	118	0.07±0.02
3	5 wt% SBM	Injected	0.88	294	1.23±0.2
		Recrystallized	0.81	402	1.45±0.2
4	10 wt% SBM	Injected	0.95	305	1.12±0.2
		Recrystallized	0.95	313	1.15±0.2
5	10 wt% SBM	Injected	0.74	323	0.73±0.2
		Recrystallized	0.91	275	0.92±0.2
6	15 wt% SBM	Injected	0.58	439	0.58±0.2
		Recrystallized	0.67	322	0.51±0.2
7	20 wt% SBM	Injected	0.82	352	0.68±0.2
		Recrystallized	0.82	343	0.67±0.2
8	20 wt% SBM	Injected	0.91	835	2.04±0.5
		Recrystallized	0.99	805	2.42±0.5

$$d = 2\sqrt{\frac{A}{\pi}} \tag{1}$$

where A is the area of the particle measured on the ultrathin section. Raw measurements obtained from TEM micrographs were corrected to obtained better estimations of the real distributions in the bulk. These corrections particularly concerned the cross-section effect which tends to overestimate the number of small particles and the projection effect due to the non-zero thickness of ultrathin sections. Details of this image analysis are given in a separate study [26].

Degree of crystallinity and nature of the crystalline phases of the PA12 matrix were studied from 2D diffraction patterns obtained by wide-angle X-ray scattering (WAXS) from a generator with a Cu Kα radiation source.

Possible degradation of the PA12 matrix and molecular weight distributions were characterized by size exclusion chromatography (SEC) in benzyl alcohol at 130 °C on a WATERS Alliance GPCV 2000 apparatus.

2.4. Impact testing

Impact response was studied by notched Charpy impact tests on an instrumented CEAST® Resil Impactor apparatus. All tests were run at room temperature with a pendulum speed at impact of 2.9 m/s. For each system, values of Charpy impact strength were calculated as averages over four to five specimens.

3. Results

Semicrystalline polyamide-12 (PA12) is toughened with various fillers: reactive ethylene–propylene rubbers (EPR*) and poly(styrene)–poly(butadiene)–poly(methyl methacrylate) block copolymers (SBM). Filler dispersions are studied by TEM and the distribution in particle size is quantified by image analysis. For all the samples, size distributions are well described by log-normal statistical laws defined by density functions of the following form:

$$f(d) = \frac{1}{2\pi s d}\exp\left[-\frac{(\ln d - m)^2}{2s^2}\right] \tag{2}$$

where d is the particle diameter and s and m are the standard deviation and number average values, respectively, of the distribution of $(\ln d)$. The number average ligament thickness, L_n, is then estimated, assuming a packing model for the particles, to be [43]:

$$L_n = d_n\left[C\left(\frac{\pi}{6\Phi}\right)^{1/3} e^{s^2} - 1\right] \tag{3}$$

where d_n is the number average particle diameter, Φ the filler volume fraction and C a packing constant chosen equal to 1.09 (body centered lattice). Interestingly, Eq. (3) shows that when the size distribution is polydisperse, L_n is not defined by d_n and Φ alone. It also depends significantly on the width of the size distribution represented by parameter s. For sake of clarity, this point is discussed in more details elsewhere [26]. Values of s, d_n and L_n are reported in Table 1 of the experimental section.

Charpy impact resistance is measured by hitting a notched test bar in well-defined conditions as schematically described in Fig. 1(a). The corresponding impact strength, J, is expressed as the energy lost by the impactor normalized by the cross-section of the test bar. The impact behavior of the injected toughened PA12 systems is very comparable to

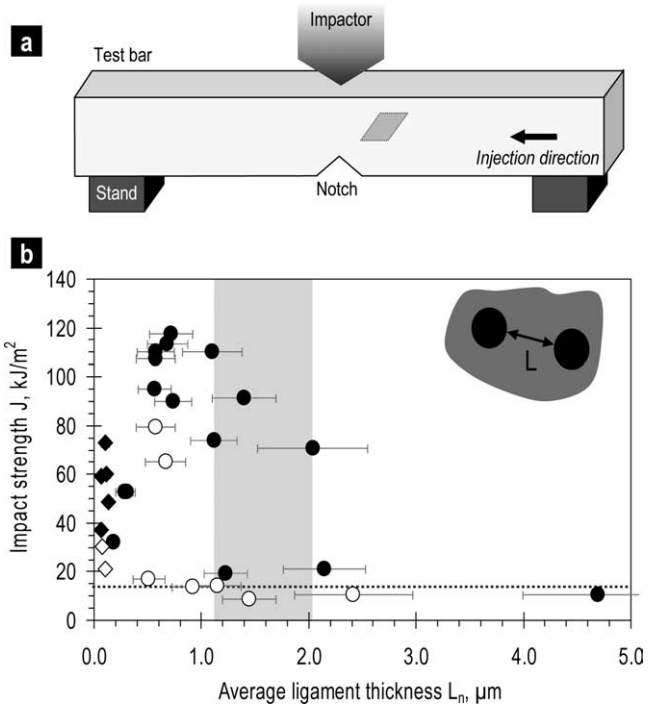

Fig. 1. Impact testing. (a). Schematic representation of Charpy impact testing. Hatched region shows the thin section observed by optical and electron microscopy in Figs. 3 and 4. (b). Notched Charpy impact strength, J, measured at 25 °C, as a function of the average interparticle ligament thickness, L_n. Impact strength values are averages of at least 4–5 samples. Error bars are the standard deviation of the distribution in ligament thickness of each sample [26]. Full symbols are obtained with injected test bars toughened with different fillers (♦ EPR*, ● SBM) at various concentrations and particle sizes. A ductile-to-brittle transition highlighted in grey occurs around a critical ligament thickness, L_c, of about 1.5 µm. Dashed line indicates the impact strength of neat PA12. As it is discussed here, data obtained after a thermal treatment (open symbols) question the existence of an intrinsic critical ligament thickness.

what is reported in the literature for other toughened semicrystalline polymers [3,17–22].

Fig. 1(b) shows the impact strength, J, of injected samples as a function of the average ligament thickness, L_n. A brittle-to-ductile transition marking the onset of toughening efficiency occurs around a critical average ligament thickness, L_c, of about 1.5 µm. Below this critical value, high toughness levels are achieved: the impact strength is increased from 15 kJ/m^2 for neat PA12 up to about 60 kJ/m^2 with EPR* and 110 kJ/m^2 with SBM particles. Like in previous studies, a rather good correlation between impact strength and matrix confinement appears over the wide range of ligament thicknesses scanned by changing the concentration and size of fillers. However, these results based on injected samples only, give no indication about the relationship that may exist between toughening efficiency and crystalline organization of the matrix.

Varying extrusion and injection conditions may change both the crystalline organization and the particle distribution. Hence, to disentangle these parameters and study the only effect of the crystalline organization, we apply a thermal treatment to injected samples. Impact test bars are melted in a mould that maintains their shape, and are then slowly cooled down to room temperature. In the following, we refer to these samples as recrystallized samples. Special care is taken to avoid degradation of the samples. Size exclusion chromatography shows no changes in the molecular weight of the PA12 matrix after the thermal treatment. Image analysis also confirms that for each system, injected and recrystallized samples have similar particle distributions and average ligament thickness, as shown in Fig. 2 for two systems toughened with EPR* and SBM particles. Indeed, the time scale of the thermal treatment is rather short compared to the slow kinetics of particle coalescence.

The thermal treatment greatly modifies the crystalline organization of the test bars as shown by optical micrographs in Fig. 3. Injected samples exhibit typical heterogeneous crystalline microstructures, as illustrated in Fig. 3(a), which are mostly determined by the flows, strong shearing and temperature gradients produced when the melted polymer enters the mould [27–30]. Several layers are distinguished through the thickness of the test bars: a skin (S), an intermediate region (I) and a core (C). The skin is only a few tens of microns wide and is highly oriented parallel to the injection direction. Most of the sample consists of an intermediate region where crystalline organization is fine and oriented along the flow lines resulting from injection. In the core, the crystalline organization is isotropic and rather coarse.

After the thermal treatment, the oriented and heterogeneous microstructures induced by injection-molding are completely erased. They are uniformly replaced by coarser isotropic microstructures as shown in Fig. 3(b). Since the thermal treatment does not induce any severe mechanical constraints, crystallization is quiescent and there is no more distinction between skin, intermediate and core regions. Impact behavior of the polymer matrix is well-known to depend on several features of the crystalline structure [31–33]. Thus, it is important to stress that, although the thermal treatment considerably changes the crystalline organization, it does not induce any significant changes in the nature of the crystalline phase nor in the degree of crystallinity as observed by X-ray scattering. The crystalline phase is the γ-phase of PA12 [34]. Depending on the systems, the degree of crystallinity is about 27–37% and for a given system, the difference between injected and recrystallized samples is less than 2–3%.

On a more microscopic scale, TEM observations of injected and recrystallized samples reveal clear differences in crystalline orientation and grain size. Samples are stained with a preparation of phosphotungstic acid which selectively stains the amorphous PA12 regions. On TEM micrographs, the PA12 matrix appears as an assembly of bright crystalline lamellae separated by thin and dark amorphous layers as shown in Fig. 4 for PA12 toughened with small EPR* and large SBM particles. In the

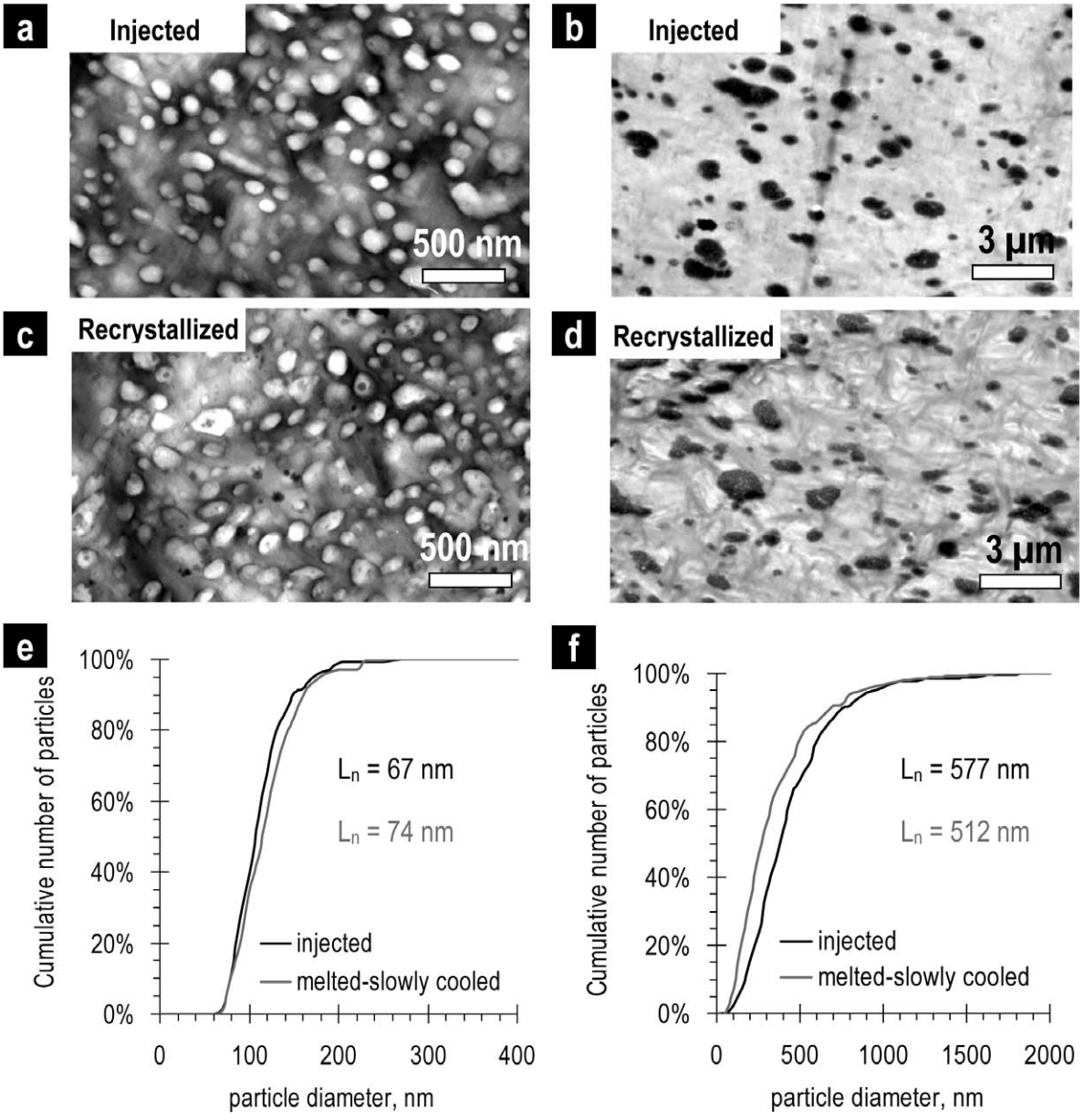

Fig. 2. Particle dispersion is preserved through the thermal treatment. TEM micrographs in injected (a) and recrystallized (c) PA12 toughened with 20% EPR*, and in injected (b) and recrystallized (d) PA12 toughened with 15% SBM. Due to staining techniques, contrast is inversed for EPR* and SBM toughened systems. The corresponding distribution in particle size and average ligament thickness, L_n, are given in e for EPR* and f for SBM particles. Very little difference is observed between injected and recrystallized samples confirming that the thermal treatment has no effect on the particle dispersion.

intermediate region of injected samples (Fig. 4(a) and (b)), the crystalline lamellae are highly correlated and extend in the same direction over several tens of microns, which is much larger than the dimensions of the micrograph. They are mostly oriented perpendicularly to the local flow direction that can be deduced from the shape of the elongated particles. This is consistent with theories of flow-induced crystallization which predict that polymer chains are aligned parallel to the flow so that they form crystalline lamellae perpendicular to it [28–30]. In contrast, recrystallized samples (Fig. 4(c) and (d)) do not exhibit any preferential orientation. Crystalline lamellae are less correlated and assembled into bundles, small grains, of a few microns in size. These observations show that the crystalline organization of the PA12 matrix strongly depends on thermo-mechanical history.

We do not observe any transcrystalline layers in the vicinity of filler particles. In particular, there are no radially oriented crystalline lamellae stemming from the surface of particles. Hence, the microscopic structure of these bulk PA12 systems differs from the picture proposed by the transcrystalline layer model. The crystalline organization consists of lamellar stacks whose orientation and length are mostly determined by processing conditions. Particles are

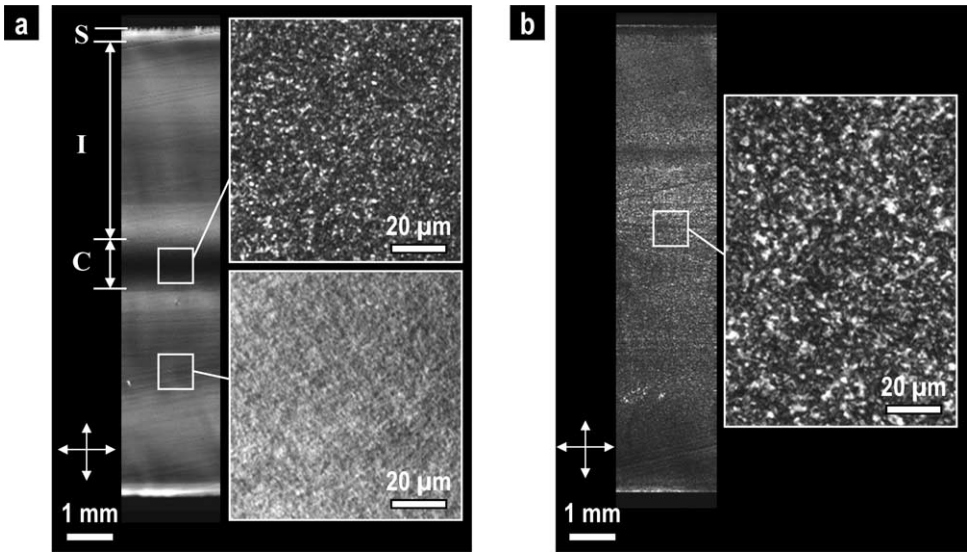

Fig. 3. The thermal treatment modifies the crystalline organization. Thin sections cut through the thickness of impact test bars are observed by optical microscopy under crossed polarizers: injected (a) and recrystallized (b) samples of PA12 toughened with 20% EPR* particles. Crossed arrows indicate the orientation of the analyzer and polarizer. Injection direction is horizontal. All injected samples like a exhibit a macroscopically heterogeneous structure with a skin (S), an intermediate layer (I) and a core (C). Recrystallized samples like b are homogeneous and macroscopically isotropic.

randomly embedded in this crystalline matrix. This seems to be the case for all PA12 systems with both small (EPR*) and large (SBM) particles.

Impact resistance and toughening are also greatly affected by the thermal treatment as shown in Fig. 5(a). All the recrystallized samples have a consistently lower impact strength than the corresponding injected ones. In neat PA12, both injected and recrystallized samples break in a brittle fashion as illustrated by pictures of post-mortem test bars in Fig. 5(b). The impact strength of the recrystallized sample is about twice lower than that of the injected one. In principle, the thermal treatment affects the amorphous phase in terms of free volume. However, in control experiments, samples have been annealed for 24 h at 150 °C (below the melting temperature but well above the glass transition temperature of PA12) and quenched at various speeds. We do not observe any appreciable effects on toughness suggesting that free volume changes within the amorphous layers do not explain the sharp drop in impact strength reported in recrystallized samples.

Injected samples toughened with 20% EPR* or 15% SBM exhibit a tough and ductile behavior with high values in impact strength. Crack propagation was stabilized and the test bars slipped through the stand before complete failure. Large whitened zones on each flank of the crack and through the whole sample thickness reveal that cavitation and extensive plastic deformation occurred in a large volume during crack propagation as shown in Fig. 5(c) and (d). After the thermal treatment, the impact strength of recrystallized samples toughened with 20% EPR* is divided by a factor 2. Still, the sample is rather tough and fracture is ductile. The case of PA12 toughened with 15% SBM is more spectacular. The thermal treatment induces a sharp drop in impact resistance. Here, the average ligament thickness, L_n, of about 500 nm is well below the critical value of L_c measured with injected samples. Yet, such ductile toughened PA12 system becomes brittle after recrystallization and about as weak as neat PA12. Hence, the toughening effects of the impact modifier can be completely annihilated by changes in the crystalline organization of the matrix.

4. Discussion

Impact tests and TEM observations of various samples suggest the following microscopic picture. It is based on the idea that voids or crazes are preferentially initiated in the amorphous phase while plastic deformation is mainly controlled by chain slips and dislocations within the crystalline lamellae. In recrystallized samples, the macroscopic isotropy and homogeneity of the matrix simplify greatly the interpretation of impact experiments. It is expected that the slow cooling rate ($\sim$1 °C/min) applied to recrystallized samples favored reeling in of polymer chains during crystallization from the melt [35,36]. Crystalline lamellae form micron-size grains having distinct orientations. Both amorphous layers and grain boundaries should be little entangled with few ‘tie chains’ bridging crystalline lamellae. As a result, stress and strain are highly localized along these regions. Microcracks or crazes can be easily initiated and the crack can propagate through these weak defects [37].

It is not clear yet whether microcracks would rather form in grain boundaries, in amorphous layers or in both types of regions. In any case, the semi-crystalline matrix can be seen

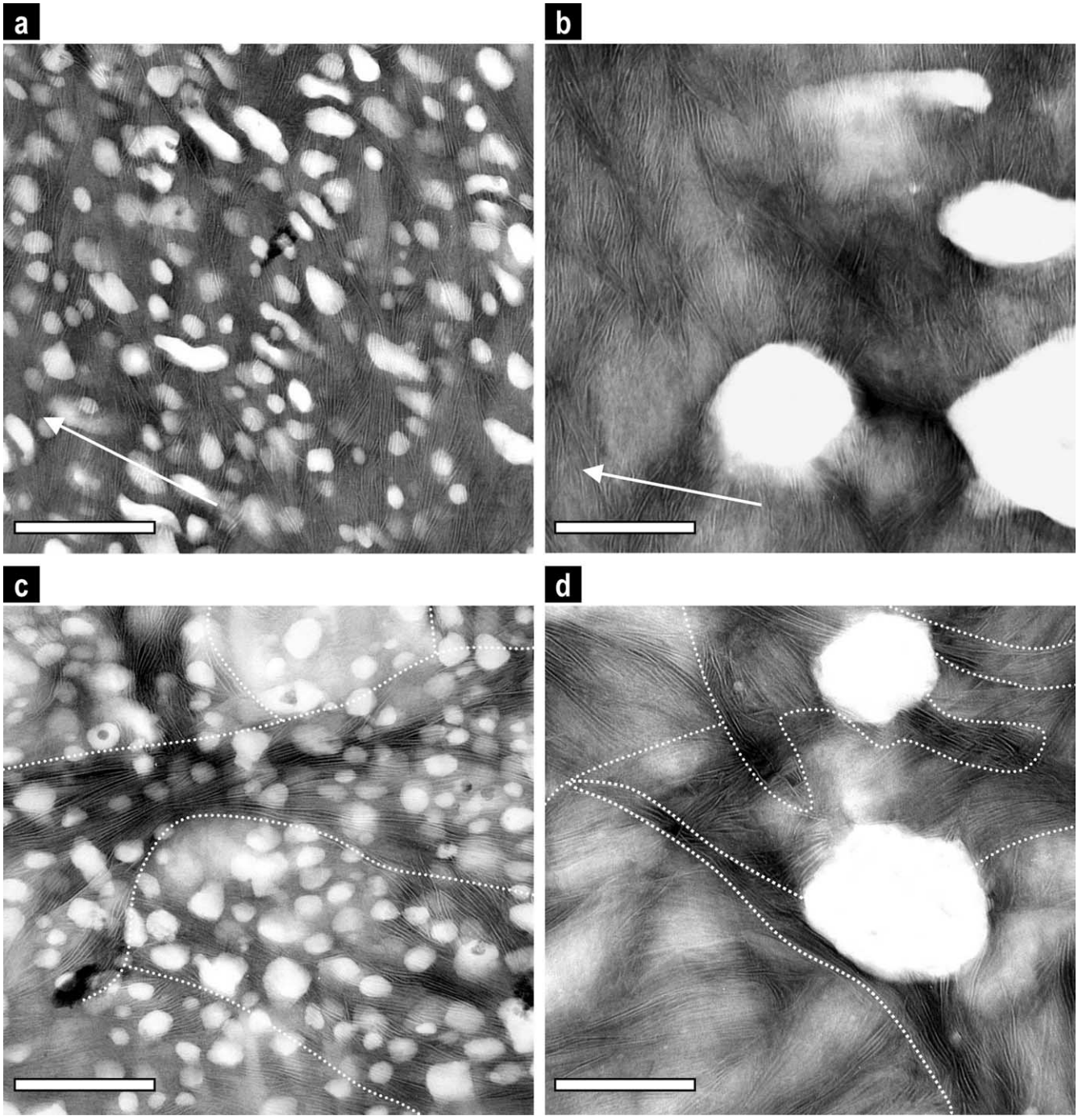

Fig. 4. TEM micrographs show the crystalline organization of the PA12 matrix. The matrix consists of alternating crystalline lamellae (bright) and amorphous layers (dark) while unstained EPR* and SBM particles are bright. Intermediate region of injected samples toughened with 20% EPR* (a) and 15% SBM (b). Arrows indicate the local direction of flow produced during injection-molding. Same region as in a and b in recrystallized samples toughened with 20% EPR* (c) and 15% SBM (d). White dotted lines outline the boundaries between grains of similarly oriented lamellae (scale bar = 500 nm).

as a network of weak interfaces which characteristic length would either be the grain size or some typical length of crystalline lamellae. The cohesive stress of these interfaces would depend on molecular parameters such as entanglement density and concentration in 'tie chains'. Interestingly, both parameters are clearly sensitive to crystallization conditions and thus, to processing history. In the following, we assume that grain boundaries are the weakest defects through which the crack can propagate.

An alternative to this brittle crack propagation is the plastic deformation of the matrix ligaments. Whether the crack propagates in a brittle way or whether its propagation is stabilized by plastic dissipation depends on the relative values of the length and cohesive stress of grain boundaries

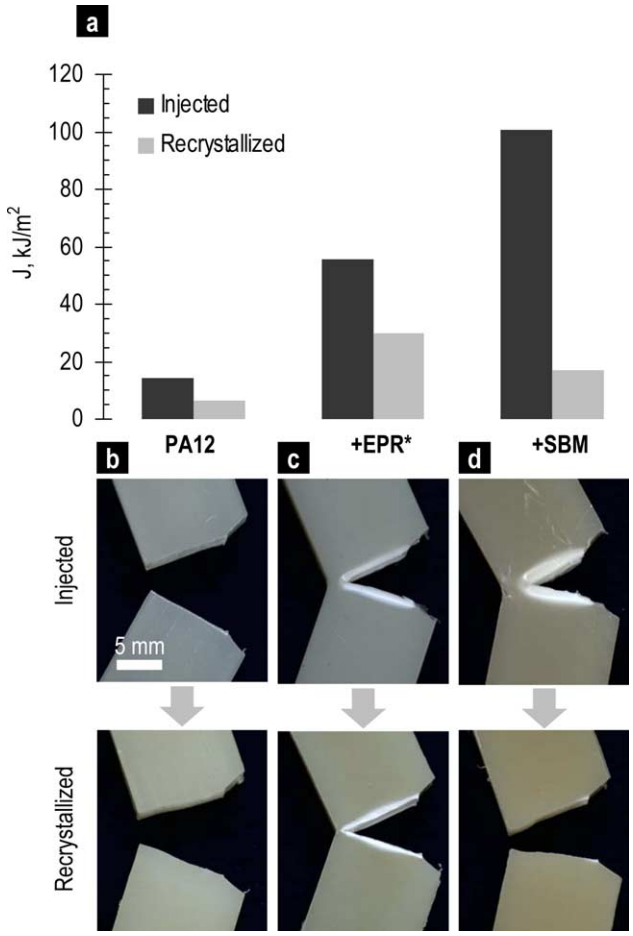

Fig. 5. Impact behavior of injected and recrystallized samples. (a) Notched Charpy impact strength, J, of toughened PA12 systems for injected and recrystallized samples. (b)–(d). Post-mortem test bars of injected (top row) and recrystallized (bottom row) samples of neat PA12 (b), PA12 toughened with 20% EPR* (c), PA12 toughened with 15% SBM (d).

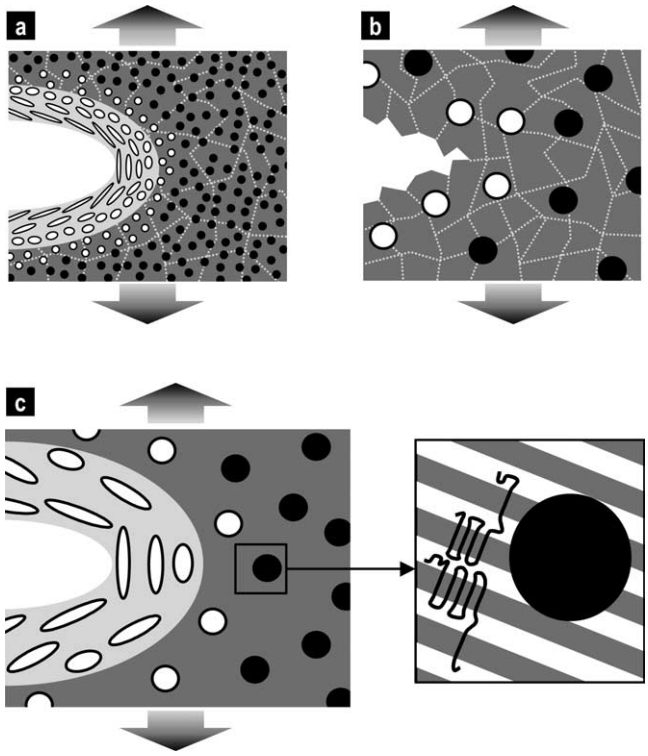

Fig. 6. A picture of toughening mechanisms. Schemes illustrate the situations encountered in recrystallized samples toughened with 20% EPR* (a) or 15% SBM (b), and in the intermediate region of these injected samples (c). Black discs correspond to the filler particles, white discs to cavitated particles. Gray dotted lines illustrate the grain boundaries in recrystallized samples. Cavitated particles are elongated in the direction of principal stress in plastically deformed zones (light grey) on each side of the cracks. Inset in c indicates the configuration of the polymer chains within the crystalline (grey) and amorphous (white) lamellae.

with respect to the ligament thickness and yield stress of the matrix. Here, we assume that particle cavitation is not a limiting factor and occurs in all cases. In other words, the stress required to create voids in particles is supposed to be lower than those necessary for brittle crack propagation or plastic deformation. This is an optimal situation. In many cases depending on particle size and structure, cavitation is not induced so easily and should be taken into consideration [3,8,9,14].

Consider the situation depicted in Fig. 6(a) for small particles. A crack propagates steadily in an infinite solid and under constant remote tensile stress. The ligament thickness is much smaller than the grain size. For given loading conditions, the matrix is so confined that the local shear stresses can be strong enough to initiate and propagate plastic deformation through the whole ligament thickness. This tough behavior occurs before brittle crack propagation is initiated in grain boundaries. It is the case of recrystallized PA12 toughened with 20% EPR* shown in Fig. 4(c). In the opposite situation illustrated in Fig. 6(b) for bigger particles, the ligament thickness is larger and comparable to the grain size. Stress field overlap and thus local shear stresses are much weaker. Hence, microcracks form and a brittle crack propagates along the grain boundaries before dissipative plastic deformation can occur through the whole ligament thickness. In this case, the presence of filler particles has no toughening effect as it is observed in recrystallized PA12 toughened with 15% SBM shown in Fig. 4(d).

In injected samples, the situation is more complex. The crystalline organization is strongly heterogeneous on a macroscopic scale. Toughening results from the combined deformation of the skin, intermediate and core regions. In the isotropic core, mechanisms are probably close to those in recrystallized samples. In the intermediate region, however, the crystalline orientation would play an important role, enabling to achieve high levels of toughness even for large ligament thickness like those encountered in the SBM toughened system shown in Fig. 4(b). Indeed, crystalline lamellae are strongly correlated over huge distances much larger than the ligament thickness as illustrated in Fig. 6(c). Unlike in recrystallized samples, these lamellae do not form distinct grains. A brittle crack here propagates through the amorphous layers. Injected test bars were quenched and

crystallized by some flow-induced mechanisms. As a consequence, entanglement density, 'tie chain' concentration and thus cohesive stress of amorphous layers are much higher than those in recrystallized samples. In addition, the oriented matrix exhibits directions of low shear yield stress due to easy chain slips perpendicularly to the crystalline lamellae [38]. Such a long distance orientation favors extensive plastic deformation and thus energy dissipation in a large volume. These interpretations together with microscopic observations strongly support recent modeling studies by van Dommelen et al. [39] who reported that a highly oriented crystalline organization can indeed induce large plastic deformation.

In summary, by applying a thermal treatment to our systems, we could substantially modify the crystalline organization of the matrix in terms of orientation and molecular structure. Such modifications had great consequences on the impact behavior since they certainly changed both the brittle strength (cohesive stress of the amorphous regions) and ductility (size and orientation of the crystalline lamellae) of the matrix [40]. Interestingly, this qualitative picture can be compared to recent works by Plummer et al. who tuned the matrix ductility by changing the temperature or moisture content [41]. The authors report that for a given particle distribution, toughening requires a certain minimum level of ductility in order to be effective, which in terms of the model proposed here, could be described as follows: the more ductile the matrix is, the easier the matrix ligament can deform plastically before a brittle crack propagates through weak amorphous regions.

5. Conclusions

Our results on toughened PA12 systems show that for a given polymer matrix and given impact conditions (temperature, speed, geometry…), the critical ligament thickness is not an intrinsic material property. The ligament thickness has to be considered in conjunction with other lengths characterizing the crystalline organization of the matrix, which in turn strongly depends on the thermo-mechanical history of the samples. These effects cannot be treated as practical complications, but seem to be essential ingredients that determine the toughness of reinforced semicrystalline polymers. Even for macroscopically isotropic and homogeneous recrystallized samples, toughening efficiency depends on crystalline organization on intermediate scales. Thus, in practice, toughening is greatly influenced by processing which induces strong crystalline heterogeneities and orientations. This is indeed well reported in industrial practice and recent model experiments for reinforced polyethylene [21,42]. As a consequence, toughening strategy and optimum particle dispersion should be adapted to processing conditions, geometry and size of the objects as well as probable impact direction. Inversely, for a given reinforced polymer material, the optimum processing and design of plastic parts should take into account the influence of orientations and correlations of the crystalline organization on impact resistance.

Acknowledgements

We are indebted to Patrick Bassoul (ESPCI) and Patrick Coupard (ARKEMA) for their help and advice on the use of microscopy. We are grateful to Michèle Milléquant, James Lesec and Sylvie Girault for SEC and X-ray analysis. We thank warmly P. Borg, H. Brown, E. Kramer, V. Rebizant, M. Rubinstein, A.-V. Ruzette, and F. Tournilhac for helpful discussions. Financial support from TOTAL and ARKEMA is gratefully acknowledged. *Competing financial interests*. The authors declare that they have no competing financial interests.

References

[1] Kinloch AJ, Young RJ. Fracture behaviour of polymers. 2nd ed. London: Elsevier Applied Science; 1985.
[2] Argon AS, Cohen RE. Toughenability of polymers. Polymer 2003;44:6013–32.
[3] Borggreve RJM, Gaymans RJ, Schuijer J, Ingen Housz JF. Brittle-tough transition in nylon–rubber blends: effects of rubber concentration and particle size. Polymer 1987;28:1489–96.
[4] Donald AM, Kramer EJ. Plastic deformation mechanisms in poly(acrylonitrile-butadiene-styrene). J Mater Sci 1982;17:1765–72.
[5] Yee AF. Proceedings of conference on toughening of plastics, London; 1985.
[6] Muratoglu OK, Argon AS, Cohen RE, Weinberg M. Toughening mechanism of rubber-modified polyamides. Polymer 1995;36:921–30.
[7] Muratoglu OK, Argon AS, Cohen RE, Weinberg M. Microstructural fracture processes accompanying growing cracks in tough rubber-modified polyamides. Polymer 1995;36:4787–95.
[8] Kayano Y, Keskkula H, Paul DR. Fracture behaviour of some rubber-toughened nylon 6 blends. Polymer 1998;39:2835–45.
[9] Kim GM, Michler GH. Micromechanical deformation processes in toughened and particle filled semicrystalline polymers. Part 2: model representation for micromechanical deformation processes. Polymer 1998;39:5699–703.
[10] van der Wal A, Gaymans RJ. Polypropylene–rubber blends: 5. Deformation mechanism during fracture. Polymer 1999;40:6067–75.
[11] Kalb F, Léger L, Creton C, Plummer CJG, Marcus P, Magalhaes A. Molecular control of crack tip plasticity mechanisms at a PP-EPDM/PA6 interface. Macromolecules 2001;34:2702–9.
[12] Fukui T, Kikuchi Y, Inoue T. Elastic–plastic analysis of the toughening mechanism in rubber-modified nylon: matrix yielding and cavitation. Polymer 1991;32:2367–71.
[13] Dijkstra K, Bolscher GHT. Nylon-6 rubber blends: 3. Stresses in and around rubber particles and cavities in a nylon matrix. J Mater Sci 1994;29:4286–93.
[14] Lazzeri A, Bucknall CB. Applications of a dilatational yielding model to rubber-toughened polymers. Polymer 1995;36:2895–902.
[15] Lazzeri A, Bucknall CB. Toughening of plastics. In: Pearson RA, Sue H-J, Yee AF, editors. ACS symposium series, vol. 759, 2000. p. 14.

[16] Tzika PA, Boyce MC, Parks DM. Micromechanics of deformation in particle-toughened polyamides. J Mech Phys Solids 2000;48: 1893–929.
[17] Wu S. Phase structure and adhesion in polymer blends: a criterion for rubber toughening. Polymer 1985;26:1855–63.
[18] Wu X, Zhu X, Qi Z. Dependence of impact strength on rubber particle concentration of PP/EPDM blends. In: Young RJ, editor. Proceedings of the eighth international conference on deformation, yield and fracture of polymers, vol. 78, 1991. p. 1–4.
[19] Oshinski AJ, Keskkula H, Paul DR. The role of the matrix molecular weight in rubber toughened nylon 6 blends: 2. Room temperature Izod impact toughness. Polymer 1996;37:4909–18.
[20] Bartczak Z, Argon AS, Cohen RE, Weinberg M. Toughness mechanism in semi-crystalline polymer blends: I. High-density polyethylene toughened with rubbers. Polymer 1999;40:2331–46.
[21] Bartczak Z, Argon AS, Cohen RE, Weinberg M. Toughness mechanism in semi-crystalline polymer blends: II. High-density polyethylene toughened with calcium carbonate filler particles. Polymer 1999;40:2347–65.
[22] Loyens W, Groenickx G. Ultimate mechanical properties of rubber toughened semicrystalline PET at room temperature. Polymer 2002; 43:5679–91.
[23] Rebizant V, Tournilhac F, Beaume F, Navarro C, Leibler L. In press.
[24] Martinez-Salazar J, Cannon CG. Transmission electron microscopy of polyamides. J Mater Sci Lett 1984;3:693–4.
[25] ImageJ software: available at http://rsb.info.nih.gov/ij/.
[26] Corté L, Leibler L. In press.
[27] Piorkowska E. Modeling of polymer crystallization in a temperature gradient. J Appl Polym Sci 2002;86:1351–62.
[28] Keller A, Kolnaar HWH. Processing of polymers. In: Meijer HEH, Cahn RW, Haasen P, Kramer EJ, editors. Materials science and technology, vol. 18, 1997. p. 191–266.
[29] Peters GWM, Swartjes FHM, Meijer HEH. A recoverable strain-based model for flow-induced crystallization. Macromol Symp 2002; 185:277–92.
[30] Kornfield JA, Kumaraswamy G, Issaian AM. Recent advances in understanding flow effects on polymer crystallization. Ind Eng Chem Res 2002;41:6383–92.
[31] Perkins WG. Polymer toughness and impact resistance. Polym Eng Sci 1999;39:2445–60.
[32] Plummer CJG. Microdeformation and fracture in bulk polyolefins. Adv Polym Sci 2004;169:75–119.
[33] Grein C, Plummer CJG, Kausch H-H, Germain Y, Béguelin Ph. Influence of β nucleation on the mechanical properties of isotactic polypropylene and rubber modified isotactic polypropylene. Polymer 2002;43:3279–93.
[34] Li L, Kock MH, de Jeu WH. Crystalline structure and morphology in nylon-12: a small- and wide-angle X-ray scattering study. Macromolecules 2003;36:1626–32.
[35] Kausch HH, Plummer CJG. The role of individual chains in polymer deformation. Polymer 1994;35:3848–57.
[36] Schrauwen BAG, Janssen RPM, Govaert LE, Meijer HEH. Intrinsic deformation behavior of semicrystalline polymers. Macromolecules 2004;37:6069–78.
[37] Kuksenko VS, Tamuzs VP. In: Fracture micromechanics of polymer materials. Dordrecht: Martinus Nijhoff Publishers; 1981. p. 61–163.
[38] Lin L, Argon AS. Rate mechanism of plasticity in the crystalline component of semicrystalline nylon 6. Macromolecules 1994;27: 6903–14.
[39] van Dommelen JAW. Micromechanics of particle-modified semi-crystalline polymers, Ph.D. Thesis, Eindhoven University of Technology; 2003.
[40] Schrauwen BAG, Janssen RPM, Govaert LE, Meijer HEH. Intrinsic deformation behavior of semicrystalline polymers. Macromolecules 2004;37:6069–78.
[41] Plummer CJG, Mauger M, Béguelin P, Orange G, Varlet J. Fracture resistance of mineral reinforced polyamide 6. Polymer 2004;45: 1147–57.
[42] Schrauwen BAG, Govaert LE, Peters GWM, Meijer HEH. The influence of flow-induced crystallization on the impact toughness of high-density polyethylene. Macromol Symp 2002;185:89–102.
[43] Wu S. A generalized criterion for rubber toughening: the critical matrix ligament thickness. J Appl Polym Sci 1988;35:549–61.